PCCP

PAPER

View Article Online
View Journal | View Issue

Cite this: *Phys. Chem. Chem. Phys.*, 2016, **18**, 21322

Computational insights into the photocyclization of diclofenac in solution: effects of halogen and hydrogen bonding†

Abdulilah Dawoud Bani-Yaseen

The effects of noncovalent interactions, namely halogen and hydrogen bonding, on the photochemical conversion of the photosensitizing drug diclofenac (DCF) in solution were investigated computationally. Both explicit and implicit solvent effects were qualitatively and quantitatively assessed employing the DFT/6-31+G(d) and SQM(PM7) levels of theory. Full geometry optimizations were performed in solution for the reactant DCF, hypothesized radical-based intermediates, and the main product at both levels of theories. Notably, in good agreement with previous experimental results concerning the intermolecular halogen bonding of DCF, the SQM(PM7) method revealed different values for *d*(Cl···O, Å) and ∠(C–Cl···O, °) for the two chlorine-substituents of DCF, with values of 2.63 Å/162° and 3.13 Å/142° for the *trans* and *cis* orientations, respectively. Employing the DFT/6-31+G(d) method with implicit solvent effects was not conclusive; however, explicit solvent effects confirmed the key contribution of hydrogen and halogen bonding in stabilizing/destabilizing the reactant and hypothesized intermediates. Interestingly, the obtained results revealed that a protic solvent such as water can increase the rate of photocyclization of DCF not only through hydrogen bonding effects, but also through halogen bonding. Furthermore, the atomic charges of atoms majorly involved in the photocyclization of DCF were calculated using different methods, namely Mulliken, Hirshfeld, and natural bond orbital (NBO). The obtained results revealed that in all cases there is a notable nonequivalency in the noncovalent intermolecular interactions of the two chlorine substituents of DCF and the radical intermediates with the solvent, which in turn may account for the discrepancy of their reactivity in different media. These computational results provide insight into the importance of halogen and hydrogen bonding throughout the progression of the photochemical conversion of DCF in solution.

Received 27th May 2016,
Accepted 4th July 2016

DOI: 10.1039/c6cp03671f

www.rsc.org/pccp

Introduction

Interest in photosensitive materials, particularly various types of pharmaceuticals, has grown recently.[1–9] Attention to the photosensitivity of drug formulations arises from several consequences that might result from their exposure to light, including loss of therapeutic potency and, more importantly, the induction of unexpected clinical states.[1,4,5] Thus, gaining insight into the photosensitivity and photoreactivity of various pharmaceutical materials is essential to ensure appropriate handling and understanding of their mechanism of action. It is important to note that photosensitive drugs exhibit different responses upon exposure to light, such as photodecomposition and specific photochemical reactions such as photocyclization.[10–12] Among pharmaceutical entities that are highly photosensitive with potential consequent hazardous properties is diclofenac (DCF) (2-[2′,6′-(dichlorophenyl)amino](phenyl)acetic acid). DCF is one of the most widely used non-steroidal anti-inflammatory drugs (NSAIDs) and is frequently prescribed for the treatment of pain and inflammation associated with various rheumatic and non-rheumatic diseases; its chemical structure is shown in Scheme 1. DCF is used extensively worldwide, and hence pronounced concern must be considered not only for its potential hazardous properties but also for its mechanism of action.[13]

It is worth mentioning that the components within media can exert striking effects on physical and chemical phenomena, including chemical reactions, and consequently can be particularly important when considering the mechanisms of various processes.[14–17] In this regard, most of the reported studies concerning the photochemical reaction of DCF have focused on elucidating the mechanism of its conversion into various photoproducts and their related biological consequences without profoundly considering the contribution of crucial factors

Department of Chemistry & Earth Sciences, College of Arts & Sciences, Qatar University, P.O. Box 2713, Doha, State of Qatar.
E-mail: abdulilah.baniyaseen@qu.edu.qa

† Electronic supplementary information (ESI) available. See DOI: 10.1039/c6cp03671f

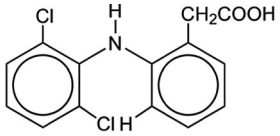

Scheme 1 The chemical structure of DCF.

in its photochemical transformation such as the non-covalent intermolecular interactions including halogen and hydrogen bonding.[2,12,13,18,19] In photochemical reactions, a significant aspect of solvent effects involves solvent/solute specific interactions such as hydrogen and halogen bonding.[20–23] For example, the photochemical oxidation of anisole can be efficiently driven by specific solvent/solute interactions, where the increase in reaction efficiency can be rationalized in terms of the hydrogen-bond donating abilities of the solvent.[20] In addition, the importance of hydrogen bonding between a substrate and free radicals was highlighted for promoting the selectivity of hydrogen atom abstraction, where an interpretation was provided that considered hydrogen-bonded complexes and their relevant effects on the reaction of concern.[21] On the other hand, because the severity of phototoxicity in biological systems can be medium- and temperature-dependent, there is a necessity to elucidate the influence of such factors on the photo-physicochemical behaviours of photosensitive drugs such as DCF. Several reports have described experimentally the effects of the medium on DCF photoconversion reactions through catalyzed and uncatalyzed processes, where the photoconversion rate was affected by the medium matrix and other physicochemical parameters of the medium.[24–30] Importantly, however, the quantification and rationalization of the influence of various medium parameters are of great significance toward gaining insights into the effects of medium on the mechanistic patterns of such photoconversion reactions; this includes not only the solvent's polarity, but also other important parameters such as specific solvent/solute interactions.

Searching the literature, it is clear that various mechanistic aspects of the DCF photoconversion have been thoroughly investigated, and consequently, and accordingly various pathways have been hypothesized; these include non-cyclization pathways and further photoconversion of the carbazole photoproducts.[12–15] However, it is essential to highlight that these discrepancies in suggested mechanisms, with the postulation of different intermediates, can be attributed to the different photochemical reaction conditions employed for conducting the experimental work. For example, it was reported that the photocyclization rate of DCF can be affected by the solvent polarity, where it was experimentally demonstrated that the rate increased as solvent polarity increases.[26] Importantly, this in turn suggests that concluding a single decisive mechanism for the photoconversion of DCF will be misleading and there is no clear evidence for a general agreement on the mechanism of the photoconversion of DCF. Thus, there is a tremendous necessity to provide additional insights into the photochemical pathways of this important drug. The objective of the present study is to shed light on the influence of solvent–solute non-covalent intermolecular interactions, namely halogen and hydrogen bonding, on the rate of the DCF photocyclization reaction in solutions through explicit and implicit semi-empirical (SQM) and density functional theory (DFT) computational investigations.

Computational details

All DFT and SQM(PM7) calculations were conducted using the Gaussian09 package[31] and MOPAC2016 software,[32] respectively. Geometries of DCF and all corresponding hypothesized intermediates and photoproducts were optimized using the DFT-B3LYP method employing the 6-31+G(d) basis set. For the DFT calculations, the solvent effects were examined implicitly using the integral-equation formalism–polarizable continuum model (IEFPCM).[33] The calculations regarding the explicit solvent effects were conducted using various orientations and numbers of solvent molecules; water molecules in particular. For the halogen-bonding effect, the explicit investigations include optimizing the geometry of DCF prior to the photochemical reaction, whereas the hydrogen bonding effect was examined for the DCF radicals before and after cyclization. All geometry optimizations were accompanied by frequency calculations. All geometries were optimized in vacuum first, and then the optimized geometries were used as input geometries for the implicit solvent effect using IEFPCM at the same level of theory noted above.

Results and discussion

It is noteworthy to mention that the photochemical behavior of DCF is comparable to that of diphenylamine (DPA). Both can undergo multi-step photocyclization reactions involving various intermediates to yield carbazole-based photoproducts. Since an early report on the photocyclization of DPA,[34] several studies have probed the pathway through which the conversion proceeds.[9,35–39] In general, one can notice that all the proposed mechanisms assert that the overall rate depends on the rate of transformation between a specific number of intermediates. The main issues that were concluded by Rahn *et al.* and supported by other researchers include the significant role of the substituent on the amine moiety and the involvement of a triplet excited-state intermediate as photocyclization proceeds.[37] However, although the pathway proposed by Rahn *et al.* is generally the most plausible, there remains a need to further clarify possible contributions from other types of intermediates, such as radicals, and intermolecular interactions with solvent molecules. Furthermore, it must be noted that DCF is an aryl halide (Ar–X) for which photodehalogenation would be expected to occur prior to the photocyclization process. Ar–X can undergo intramolecular photoreactions through two possible mechanisms: hemolysis and electron transfer, both of which involve an aryl radical ($Ar^{\bullet}$) intermediate.[39] Thus, considering the expected behaviors of DCF as an analogue of both DPA and Ar–X, the DCF photoconversion pathway and cyclization mechanism were hypothesized as depicted in Scheme 2.

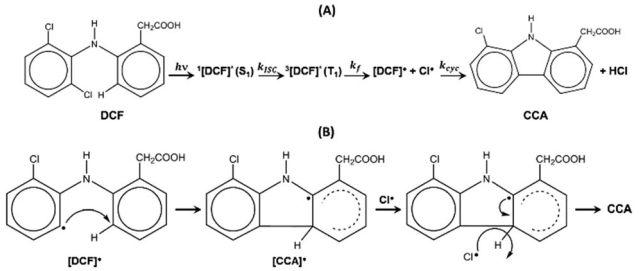

Scheme 2 (A) Major photoconversion pathway of DCF into CCA. (B) Proposed cyclization mechanism.

As illustrated in Scheme 2, upon photoexcitation, DCF can form the singlet excited state ^{1}[DCF](S1), which can then undergo an intersystem crossing process to form the triplet excited state ^{3}[DCF](T1). Then, ^{3}[DCF](T1) is dehalogenated to yield the DCF radical (DCF$^\bullet$) and chlorine radical (Cl$^\bullet$). DCF$^\bullet$ cyclizes to form the CCA radical (CCA$^\bullet$), followed by hydrogen radical abstraction by Cl$^\bullet$ to form CCA. Correspondingly, the increase of the DCF reaction rate in solvents of increasing polarity can be interpreted in terms of the increased efficiency in stabilizing/destabilizing the reactant and intermediates, namely DCF, and DCF$^\bullet$ and CCA$^\bullet$, respectively, and consequently influencing the DCF photoconversion rate. Thus, the observed influence of the solvent on the photochemical conversion of DCF is presumably caused by its effect on the rates of formation of the radicals and cyclization processes.[23,26] We hypothesize that DCF can intermolecularly interact with the solvent molecules not only through hydrogen bonding but also through halogen bonding, which in turn affects the rate of photochemical conversion of the drug.

Implicit solvent effects

Computational investigation of the solvent effects on the geometrical properties of DCF and the corresponding radical intermediates and photoproducts was conducted. The optimized geometries of DCF, DCF$^\bullet$, CCA$^\bullet$, and CCA in water, obtained using DFT/6-31+G(d) coupled with the IEFPCM method, are displayed in Fig. 1. The relevant geometrical properties of these compounds are compiled in Tables S1–S5 (ESI†); these include the bond length and charges of selected atoms and bonds that are majorly involved in the DCF photocyclization reaction.

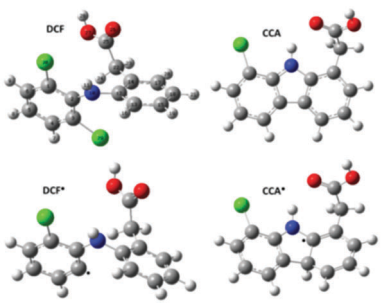

Fig. 1 Optimized geometries of DCF, DCF$^\bullet$, CCA$^\bullet$, and CCA. The calculations were conducted employing the DFT/6-31+G(d)/IEFPCM (water) level of theory.

As shown in Fig. 1, DCF appears to exhibit a geometry that is comprised of a secondary amine group with the phenyl group twisted out-of-plane with a dihedral angle (C2, C3, C12, C13) of approximately $-92 \pm 2^\circ$ in all solvents. Likewise for DCF$^\bullet$, but with minor changes. In contrast, dihedral angles of $+8^\circ$ and 0° are observed for CCA$^\bullet$ and CCA, respectively. These changes in the dihedral angles indicate the importance of minimizing the twist angle as a precyclization step. Hence, the nonplanarity in the structure of DCF implies the necessity for intramolecular rotation for ring closure to occur as a major step in the DCF photocyclization pathway to yield the carbazole derivative with a planar geometry. Notably, the increase in the rate of the DCF photochemical reaction with increasing solvent polarity can be supported by examining the calculated dipole moment (μ) of each substance using the DFT-B3LYP/6-31+G(d)/IEFPCM method. The μ values for DCF, DCF$^\bullet$, CCA$^\bullet$, and CCA calculated in water are 2.48, 2.74, 2.55, and 3.36 Debye, respectively. Notably, the intermediates and the product have higher μ values relative to the parent molecule. Such increases in μ as a result of the DCF photoconversion can be interpreted in terms of the enhanced efficiency of localized charge stabilization in the polar solvent, and consequently an increase in the overall reaction rate.

This can be further supported by evaluating the change in the charges of selected atoms involved in the cyclization process. See below for further discussion and examples.

Intermolecular halogen bonding

Recently, interest in elucidating the importance of halogen bonding (XB) as a non-covalent intramolecular and intermolecular interaction has grown considerably.[40–44] It has been demonstrated experimentally and computationally that XB exists in a wide spectrum of systems including organic and biological systems.[40–44] In principle, the XB of the type R–X$\cdots$Y–R′ has a significant role in drug activity and reactivity.[43,44] With respect to the arrangement R–X$\cdots$Y–R′, X (X: Cl, Br, I) and Y are defined as the XB donor and acceptor, respectively. Examining the structure of DCF, one can see that DCF can interact intermolecularly with the solvent molecules not only through hydrogen bonds *via* the amine (–NH_2) and carboxylic acid (–COOH) moieties, but also through XBs *via* the two chlorine substituents. For the latter, we thus believe that such types of intermolecular interactions may play significant roles in the photocyclization reaction of DCF as a pre-process that occurs prior to the photodehalogenation step. Hence, the effect of solvent polarity on the two C–Cl bonds, namely C1–Cl30 and C3–Cl29, was implicitly examined *via* optimizing the geometry of DCF in selected solvents of different polarity, namely, water, ethanol, isopropanol, dichloromethane, ethyl acetate, 1,4-dioxabe, and *n*-hexane. It must be mentioned that although the implicit computations do not fully reflect the extent of halogen bonding, such calculations provide insight into how halogen bonding affects the charge density of carbon and chlorine atoms as well as the C–Cl bond length (d_{C-Cl}), which in turn suggests trends in reactivity. Three methods of charge density analyses were conducted, namely Mulliken (MQ), Hirshfeld (HQ) and Natural Bond Orbital (NBO). All calculated geometrical parameters in different solvents are compiled

Table 1 Calculated geometrical and atomic properties of DCF in different media

	C1–Cl30							C3–Cl29						
		Charges							Charges					
		C1			CI30				C3			CI29		
Medium	B.L. (A)	M.Q.	H.Q.	NBO	M.Q.	H.Q.	NBO	B.L. (A)	M.Q.	H.Q.	NBO	M.Q.	H.Q.	NBO
Vacuum	1.765	−0.5813	0.0077	−0.0795	0.1147	0.0392	0.0032	1.758	0.6923	0.0104	−0.0871	0.1036	−0.0368	0.0190
Water	1.765	−0.9327	0.0063	−0.0774	0.0800	−0.0467	−0.0018	1.762	0.6988	0.0083	−0.0900	0.1296	−0.0527	0.0043
Ethanol	1.765	−0.9114	0.0061	−0.0779	0.0786	−0.0460	−0.0018	1.762	0.7173	0.0079	−0.0906	0.1318	−0.0523	0.0047
Isoprop.	1.766	−0.8962	0.0061	−0.0782	0.0778	−0.0458	−0.0019	1.762	0.7269	0.0079	−0.0907	0.1327	−0.0523	0.0047
DCM	1.766	−0.8463	0.0058	−0.0790	0.0751	−0.0448	−0.0018	1.762	0.7653	0.0076	−0.0913	0.1376	−0.0515	0.0057
Ethyl. Ac.	1.766	−0.8046	0.0057	−0.0796	0.0730	−0.0440	0.0016	1.762	0.7968	0.0075	−0.0916	0.1420	−0.0507	0.0066
1,4-Dioxane	1.765	−0.6585	0.0076	−0.0789	0.1148	−0.0427	0.0007	1.760	0.6469	0.0097	−0.0868	0.0924	−0.0428	0.0131
n-Hexane	1.765	−0.6438	0.0076	−0.0790	0.1142	−0.0421	0.0011	1.759	0.6562	0.0099	−0.0869	0.0947	−0.0417	0.0142

in Table 1. The polarization of a covalent bond, *e.g.* C–Cl, is relatively evaluated as the difference in charge density ($\Delta Q = Q_C - Q_{Cl}$). All calculated values of ΔQ in different solvents are compiled in Table 2. Importantly, it is noteworthy mentioning that the more positive charge on the halogen atom, the stronger halogen bonding;[40–44] on the other hand, the shorter d_{C-Cl}, the more polarized bond, and consequently stronger interaction with the XB acceptor. Examining Tables 1 and 2, one can notice that C3–Cl29 is more polarized than C1–Cl30 according to the NBO and HQ analysis, which in turn is consistent with the difference in the bond length as $d_{C3-Cl29}$ is less than $d_{C1-Cl30}$. Furthermore, examining ΔQ and d_{C-Cl} across the tested solvents, it can be noted that the two C–Cl bonds are not equivalent in terms of polarization and d_{C-Cl}, where C3–Cl29 is more influenced by medium polarity, which in turn may account for the faster photoconversion observed in polar solvents.

Importantly, a more descriptive illustration of the non-covalent intermolecular halogen bonding between the solvent molecules and DCF can be obtained by conducting explicit computations. In principle, the threshold length for R–X···Y–R′ is defined as the sum of the two van der Waals radii of the atoms involved in the halogen bonding, namely X and Y, where the strength of the halogen bond is inversely proportional to the bond length.[40] Furthermore, the angle of the halogen bond ∠(R–X···Y) has a tendency to be arranged linearly for the R–X···Y with an angle of approximately 180°.[40] It must be mentioned that it is not unusual for DCF to form a network of intermolecular interactions comprised of halogen and hydrogen bonding with solvent molecules, as demonstrated by X-ray crystallography.[45] For the DCF–water interaction, a bond length (Cl···O) and angle (∠C–Cl···O) of 2.8 Å and 158.1°, respectively, were reported.[45]

In this study, with respect to DCF–solvent interactions, we focus only on water as the medium of concern. Hence, for the system of interest the halogen bond is defined as C–Cl···O–R with a threshold length of 3.27 Å, which is the sum of the van der Waals radii of the chlorine and oxygen atoms. As illustrated in Fig. 2, two potential halogen bonds may form, namely C1–Cl30···O–R and C3–Cl29···O–R. The geometry of DCF indicates that there are two orientations for the chlorine substituents with respect to the amine functional group.

For simplicity, a description of a *cis* orientation will be given for the chlorine substituent that is in the same direction as the amine group and a *trans* orientation will be used for the other chlorine substituent. As a reference scenario, two solvent molecules were manually introduced close to the chlorine atoms of the optimized DCF geometry in vacuum at a distance of approximately 3.0 Å. The optimization was then initiated without imposing any constraints. Two computational methods were employed for this purpose: DFT/B3LYP(631G+(d) and SQM(PM7). Examining the structure of DCF, one can see that the presence of the amine and carboxylic acid groups accelerate strong hydrogen bonding with the protic polar solvent that is very competitive for establishing halogen bonding. Thus, employing a computational method with dispersion forces is essential to

Table 2 Calculated ΔQ of C–Cl bonds of DCF in different media

	C1–CI30			C3–CI29		
Medium	ΔQ(M)	ΔQ(H)	ΔQ(NBO)	ΔQ(M)	ΔQ(H)	ΔQ(NBO)
Vacuum	−0.696	−0.032	−0.083	0.589	0.047	−0.106
Water	−1.013	0.053	−0.076	0.569	0.061	−0.094
Ethanol	−0.990	0.052	−0.076	0.585	0.060	−0.095
Isoprop.	−0.818	0.052	−0.076	0.594	0.060	−0.095
DCM	−0.921	0.051	−0.081	0.628	0.059	−0.097
Ethyl. Ac.	−0.878	0.050	−0.081	0.655	0.058	−0.098
1,4-Dioxane	−0.773	0.050	−0.080	0.555	0.053	−0.100
n-Hexane	−0.758	0.050	−0.080	0.562	0.052	−0.101

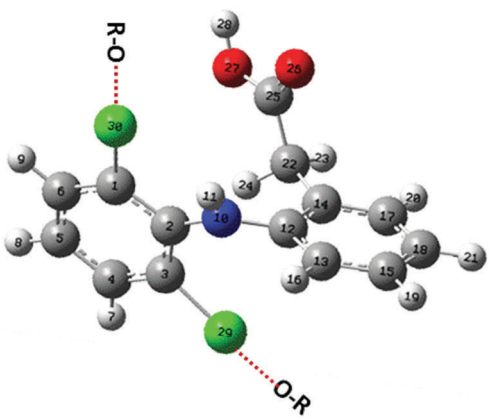

Fig. 2 Description of the DCF–Cl···O–R halogen bonding.

obtain computational results of acceptable accuracy. For the DFT investigations, two scenarios were examined, namely the explicit interaction with two and four water molecules. For both scenarios, the obtained results revealed values for d(Cl···O) and ∠(C–Cl···O) that are higher than the threshold values to be considered as strong halogen bonding. Moreover, increasing the number of water molecules did not substantially enhance the bond length and angle values, but a dramatic increase in the computational cost was noted. In fact, examining the optimized geometry of all systems, one can see that the water molecules accumulate to form a cluster around the amine and carboxylic acid groups, reflecting the competency of hydrogen bonding *versus* halogen bonding. It is noteworthy mentioning that SQM(PM7) has recently gained interest as a convenient method to examine the presence of both hydrogen and halogen bonding.[32] Notably, for the SQM(PM7) method, adding more water molecules changed the orientations of the water molecules around the whole molecule of DCF. As depicted in Fig. 3, with a total number of 20 water molecules, the obtained results revealed that both chlorine atoms can be located at a distance from the oxygen atom of the water molecules that permits halogen bonding. For the *trans* orientation, values of 2.63 Å and 162° were obtained for d(Cl···O) and ∠(C–Cl···O), respectively, whereas respective values of 3.13 Å and 142° were obtained for the *cis* orientation. Compared with the reported experimental values,[45] the calculated d(Cl···O) and ∠(C–Cl···O) of the *trans* orientation are in good agreement with these values. These results demonstrate the non-equivalency of the intermolecular interactions of the two chlorine atoms, which in turn may be interpreted as higher reactivity of one chlorine atom over the other. This can be further supported by calculating the atomic charges for both chlorine atoms. At a low level of intermolecular interaction (*i.e.*, a small number of solvent molecules), an atomic charge in the range of −(0.04–0.08 au) was obtained for both chlorine atoms. However, with 20 water molecules, charges of the chlorine atoms of approximately +0.028 and −0.121 au were obtained for the *trans* and *cis* orientations, respectively. We believe that this discrepancy in halogen bonding capacity with the solvent molecules may enhance the potential of the chlorine radical to dissociate during the photochemical conversion of DCF.

Explicit hydrogen bonding effects

The IEFPCM model considers the polarizability of the medium without accounting for any specific interaction between the solute and solvent molecules. Thus, it is necessary to apply another approach. In particular, an explicit solvent model (ESM) can facilitate the evaluation of such specific interactions that can assist gaining greater insights into the photochemical conversion of DCF. On the other hand, electrostatic potential surfaces (EPSs) can be employed for predicting the locations of charge distributions across a molecules, where positive and negative zones are most likely feasible to act as the H-bond donor and acceptor, respectively.[46–48] In this context, to support the proposed hydrogen-bonding effect on stabilizing the pre-cyclization H-bonded complex (solvent/DCF•), three approaches were considered as displayed in Fig. 4. The first two approaches involve placing one water molecule either close to the carbon radical (scenario A) or between the amine and carboxyl group

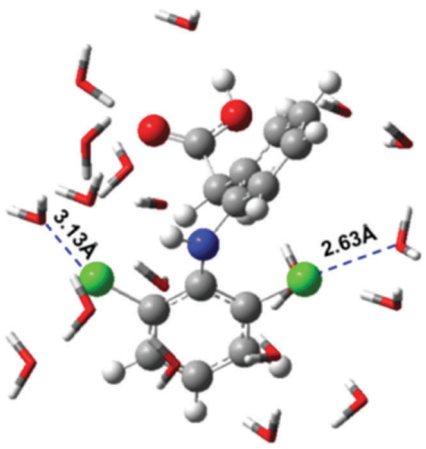

Fig. 3 SQM(PM7) optimized geometry of DCF in the explicit presence of 20 water molecules.

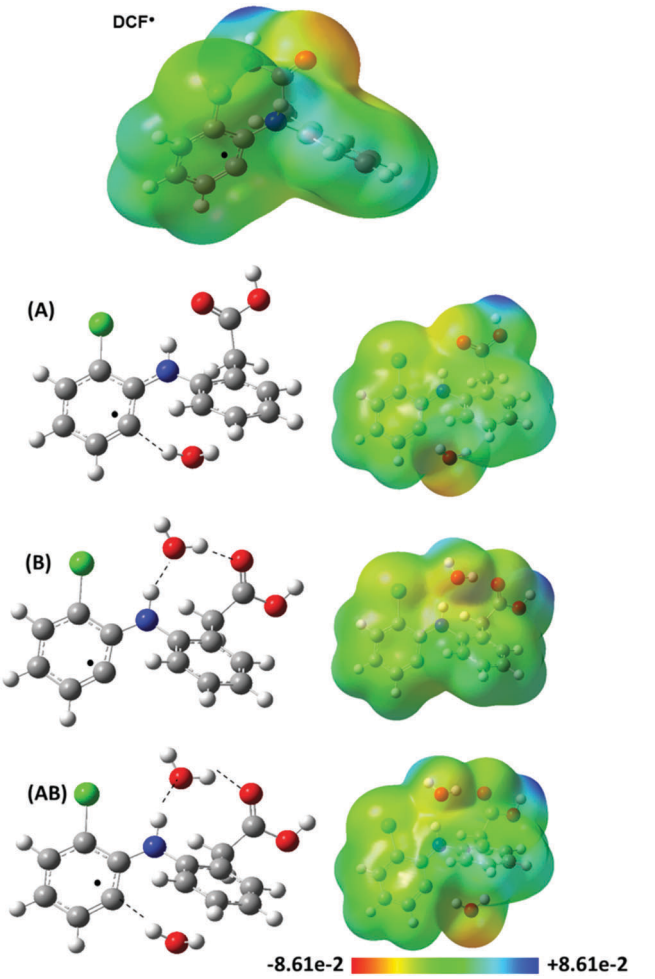

Fig. 4 (left) Three proposed explicit interactions of H_2O molecules with DCF•; (right) the corresponding electrostatic potential surfaces.

(scenario B), whereas the third approach is a combination of scenarios A and B, namely scenario AB. Correspondingly, the ESP surfaces were calculated for these three arrangements as well as for individual DCF$^{\bullet}$; results are depicted in Fig. 4. All DFT/631G+(d) calculations were conducted with and without the IEFPCM solvent method. The major geometrical parameters for DCF$^{\bullet}$ with the three arrangements are given in Table 3. Examining the ESP of DCF$^{\bullet}$, one can notice the green-yellowish zone located close to C3 indicating relatively negative charge density and hence high potentiality of acting as an H-bond acceptor. This observation is consistent with the HQ density of −0.028 and −0.030 au calculated for C3 in vacuum and water, respectively. For the adducts A, B and AB, the clear presence of red zones located close to oxygen atoms of both DCF$^{\bullet}$ and water molecules is indicative of the high charge density which enables them to act as strong hydrogen bond acceptors. Considerably, elucidation of the effect of hydrogen bonding may be linked to the intermolecular hydrogen bonding between the amino proton and the solvent molecules. In principle, the formation of intermolecular hydrogen bonds will elongate the N–H bond and reduce the charge density over the nitrogen atom, which would be offset by the carbon atom in the N–C bond. This, in turn, may increase the partial positive charge exhibited by the carbon atom, where such a behavior may favorably lead to hydrogen abstraction (H16) as a key step in the formation of a more stable intermediate, which can then lead to ring closure and the formation of CCA. Hence, solvents with high hydrogen-bond-accepting capability can increase the DCF photocyclization step, whereas the opposite effect will be observed when increasing the hydrogen-bond-donating capability.

Consequently, as mentioned above, the cyclization process is facilitated by a rotation in the C3–C2–C12–C13 dihedral angle from approximately −92° in DCF to approximately 0° in CCA. As can be inferred from Table 3, the major changes in the optimized geometry of DCF$^{\bullet}$ resulting from the inclusion of explicit water molecules are the reduction in the C3–C2–C12–C13 dihedral angle from approximately −92° to −40° as well as the effect on the charges of atoms that contribute directly to the DCF cyclization process. Without the inclusion of an explicit water molecule between the amine and carboxyl groups, the O26···H11 distance is approximately 3.8 Å, which indicates a relatively weak H-bond. Indeed, the explicit water molecule forms a bridge of H-bonds *via* N–H11···OH_2 and C22–O26···H–OH, where DCF acts as both H-bond donor and acceptor, respectively. The calculated values for the N10–H···OH_2 and O26···HOH H-bond distances are 1.86 and 1.77 Å, respectively, which is indicative of strong hydrogen bonding. Additionally, MQ, HQ and NBO charge density analyses were performed to examine the effect of hydrogen bonding on the charge density of the main atoms involved in the photocyclization process. The results obtained using the NBO method are summarized in Table 3, whereas the results of MQ and HQ analyses are summarized in Table S5 (ESI†). Interestingly, in Table 3, one can notice the significant change in the charge density induced by the presence of hydrogen bonding. The NBO analysis revealed that the biggest change in charge density was observed for C3$^{\bullet}$, where an average change of ∼0.050 au was calculated for scenarios A and AB. As can be noted, scenario B has a minor effect on C3$^{\bullet}$. Likewise, average changes in charge density for scenarios A and AB of ∼0.010, 0.011, 0.012, 0.009, 0.030, 0.010 and 0.010 au were obtained for C2, C12, C13, N10, H11, H16 and O26, respectively. This to say, the NBO analysis supports the formation of H-bond between DCF$^{\bullet}$ and protic polar solvent molecules through C3$^{\bullet}$. Consequently, as noted in Scheme 2,

Table 3 Geometrical and IR spectroscopic properties of DCF$^{\bullet}$ H2O/DCF$^{\bullet}$ H-bonded complexes (A,B, and AB)

		A		B		AB		DCF$^{\bullet}$	
Property		ESM	ESM + IEFPCM	ESM	ESM + IEFPCM	ESM	ESM + IEFPCM	Vacuum	IEFPCM
Bond lengths (Å)	C2–C3	1.394	1.396	1.403	1.404	1.405	1.406	1.392	1.391
	C13–H16	1.085	1.085	1.084	1.085	1.085	1.085	1.087	1.087
	N10–H11	1.018	1.017	1.028	1.027	1.029	1.028	1.013	1.014
	N10–C12	1.407	1.409	1.424	1.430	1.424	1.429	1.432	1.432
	C12–C13	1.405	1.406	1.410	1.409	1.410	1.409	1.398	1.400
	C3/C13	3.011	2.982	3.051	3.120	3.076	3.076	3.718	3.800
	O26/H11	2.046	2.066	3.677	3.585	3.672	3.596	3.390	3.751
Dihedral angle (°)	C3–C2–C12–C13	−41	−37	−52	−56	−55	−53	−89	−94
	C2–N10–C12–C13	−36	−32	−49	−56	−51	−54	−94	−101
Charge (NBO)	C2	0.068	0.072	0.062	0.062	0.069	0.073	0.062	0.058
	C3	0.079	0.059	0.129	0.118	0.075	0.061	0.122	0.115
	C12	0.164	0.162	0.164	0.147	0.156	0.144	0.147	0.143
	C13	−0.253	−0.259	−0.238	−0.241	−0.239	−0.242	−0.230	−0.243
	N10	−0.632	−0.625	−0.659	−0.665	−0.657	−0.658	−0.653	−0.651
	H11	0.463	0.459	0.486	0.481	0.488	0.483	0.442	0.446
	H16	0.257	0.260	0.262	0.267	0.264	0.270	0.248	0.257
	O26	−0.627	−0.657	−0.619	−0.644	−0.620	−0.642	−0.605	−0.648
IR ν (cm^{-1})	N10–H11	3501	3507	3329	3332	3309	3313	3586	3568
	C25═O26	1796	1756	1691	1659	1689	1659	1823	1775
μ (debye)		2.026	3.414	2.539	3.883	2.670	3.526	1.858	2.737

C3• has a major contribution in the cyclization process of DCF, and hence it is expected that the H-bond donating capability of the solvent has a major contribution in the photocyclization reaction of DCF.

Furthermore, the presence of hydrogen bonding can be noticed by examining the changes that may accompany its formation including its dynamics in the excited states.[49–51] It has been ascertained that the formation of hydrogen bonds would be accompanied by the lengthening of the donor bond, X–H, *e.g.* N10–H11 of DCF, which in turn can be evidenced through changes in the infrared (IR) stretching frequencies.[49,52–54] Hence, IR spectroscopy is commonly utilized experimentally and computationally for probing the strength of intramolecular and intermolecular hydrogen bonding.[53,54] Indeed, the formation of H-bonded complexes with carbon radicals as H-bond acceptors (O–H···C•) is not uncommon.[53] In his study of alkyl radicals as hydrogen bond acceptors, Hammerum reported the effect of hydrogen bonding on the length of N–H and O–H and their corresponding IR stretching frequencies, where in some cases a red shift of more than 2000 cm^{-1} was observed for N–H accompanied by a change in the bond length of N–H of different complexes in the range of 0.021–0.040 Å.[53]

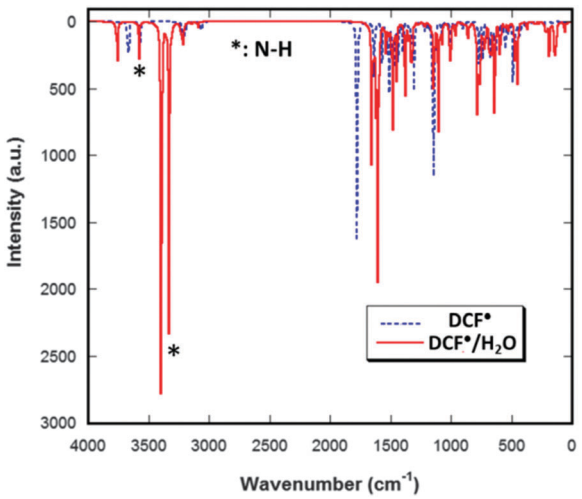

Fig. 5 Simulated IR spectra of DCF• and DCF•/H_2O; DFT/6-31+G(d)/IEFPCM (water).

In this context, the formation of H-bond between DCF• and H_2O molecules is further supported by the results of IR spectroscopy of individual and water-complexed DCF•. The simulated IR spectra of DCF• and H_2O/DCF• (as complex B) are displayed in Fig. 5. Upon examination of Table 3 and Fig. 5, it can be noted that hydrogen bonding causes an increase in the N10–H11 bond length by 0.0136 and 0.0125 Å for the AB and B adducts, respectively, with red-shifts in the vibrational frequencies of 236 and 255 cm^{-1}, respectively. For the A adduct, an increase in the O–H bond length of 0.0053 Å with an IR red-shift of 85 cm^{-1} is observed. It is essential to note that IR spectroscopy herein is utilized mainly for propping the intramolecular hydrogen bonding of the H_2O/DCF• system. Consequently, the formation of the N–H11···OH_2 H-bond does not only affect the N10–H11 bond, but also other atoms/bonds involved in the cyclization step of DCF. As mentioned above, the cyclization step is accomplished by the bonding of C3 with C13 (Scheme 2). Interestingly, the hydrogen bonding reduced the distance between C3 and C13 by approximately 0.80 Å. Taking these results to support the formation of H-bonds, one can infer that hydrogen bonding is an important factor in addition to the medium polarity for controlling the rate of the DCF photochemical reaction.

Additionally, DFT-B3LYP/6-31+G(d)/IEFPCM calculations were performed to quantitatively access the relative ground-state energies of all compounds involved in the proposed mechanism and calculate the corresponding thermodynamic parameters for each step. The results are compiled in Table 4. All calculated values are relative to DCF in the gas phase. Fig. 6 illustrates the relative electronic energy diagrams for the photoconversion of DCF into CCA + HCl in selected media. Examining Table 4 and Fig. 6, these results reveal that the products of the photodehalogenation (DCF• and Cl•) and cyclization (CCA• and Cl•) steps are ~82 and 60 kcal mol^{-1} higher in energy than DCF, respectively, whereas the products of the final step, CCA + HCl, are ~20 kcal mol^{-1} lower in energy than DCF. In addition, for the first two steps, the energy gap increases slightly as the medium polarity and hydrogen-bonding capability increases.

In the same context, the photodehalogenation of DCF into DCF• and Cl• is an endothermic and non-spontaneous process with an enthalpy change (ΔH°) of approximately + 80 kcal mol^{-1} and a Gibbs free energy change (ΔG°) of approximately +72 kcal mol^{-1}. Notably, the cyclization process from DCF• into CCA• is exothermic

Table 4 Energy and thermodynamic quantities (kcal mol^{-1}) for the photoconversion of DCF into CCA + HCl calculated using the DFT/B3LYP/6-31+G(d)/IEFPCM method

	DCF			DCF* + Cl*			CCA* + Cl			CCA + HCl		
Medium	ΔG	ΔH	ΔE_{Total}	ΔG	ΔH	ΔE_{Total}	ΔG	ΔH	ΔE_{Total}	ΔG	ΔH	ΔE_{Total}
Vacuum	0.00	0.00	0.00	71.15	80.93	82.41	50.41	57.19	58.52	−34.73	−27.58	−20.48
Water	−9.22	−9.56	−9.21	62.60	72.01	73.62	42.96	49.87	51.44	−44.11	−36.17	−29.44
Ethanol	−8.76	−9.14	−8.79	63.04	72.46	74.05	43.34	50.23	51.77	−43.68	−35.74	−29.03
Isoprop.	−8.56	−8.96	−8.62	63.23	72.63	74.23	43.48	50.37	51.91	−43.50	−35.56	−28.86
DCM	−7.75	−8.14	−7.82	64.12	73.51	75.10	44.21	51.07	52.58	−42.62	−34.71	−28.03
Ethyl. Ac.	−7.12	−7.47	−7.16	64.85	74.25	75.82	44.82	51.65	53.15	−41.87	−33.98	−27.32
Dioxane	−3.46	−3.39	−3.29	67.74	76.67	78.78	47.31	53.52	55.52	−38.73	−30.90	−24.32
Hexane	−2.85	−2.79	−2.70	68.34	77.92	79.43	47.86	54.66	56.06	−38.02	−30.21	−23.64

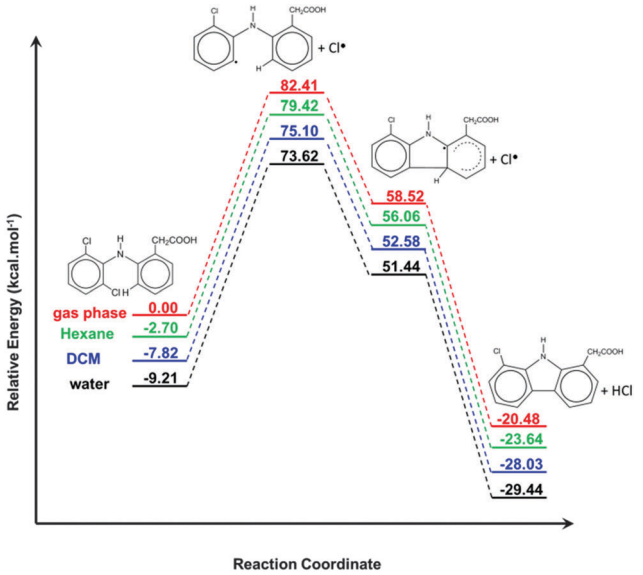

Fig. 6 Quantitative relative electronic energy diagram for the photoconversion of DCF into CCA in selected media calculated at the DFT/6-31+G(d)/IEFPCM level of theory; all values are relative to DCF in the gas phase.

and spontaneous, with ΔH° and ΔG° values near -23 and -20 kcal mol^{-1}, respectively. For the overall reaction, it can be inferred that the photochemical conversion of DCF into CCA + HCl is an exothermic and spontaneous process, with ΔH° and ΔG° of approximately -27 and -35 kcal mol^{-1}, respectively. Furthermore, there is a slight decrease ($\sim$4%) in ΔH° for the photoreaction with increasing solvent polarity. This may be attributed to the relative difference in the polarity of DCF and CCA, as concluded from the difference in the dipole moments listed in Tables S1 and S3 (ESI†). DCF and CCA exhibit changes in their dipole moments of 0.753 and 0.574 Debye, respectively, on proceeding from water to *n*-hexane as medium of the reaction, where partial compensation for the energies to cleave the intramolecular and intermolecular hydrogen bonds may be anticipated.

Conclusions

DFT and SQM computational investigations were successfully employed to explore the effects of noncovalent intermolecular interactions, namely halogen and hydrogen bonding, on the photoconversion of DCF in solution. Notably, we demonstrated that not only did the DCF photocyclization reaction rate depend on solvent polarity but also that the solvent's halogen- and hydrogen-bonding capability may contribute to the overall rate. Specifically, it was observed that the two chlorine substituents of DCF exhibit different potentials for intermolecular interactions with the medium. These differences suggest distinct reactivity of these atoms in different solvents, which may increase as the solvent's halogen- and hydrogen-bonding capability increases. The DFT calculations demonstrated that the polarities of the intermediates were higher than the parent molecule (DCF) and could thus be more efficiently stabilized in polar solvents with hydrogen bonding capability. This would correspondingly increase both the rate of their formation and the overall rate of the DCF photochemical conversion. In addition, the DFT calculations revealed that H-bonded complexes of the types (O–H$\cdots$C$^\bullet$), (N–H$\cdots$O), and (O–H$\cdots$O) can be formed, which can apparently affect the reaction rate. We believe that the findings of this study will enhance our understanding of DCF photoconversion, which is particularly important to further understand the photobehavior of relevant biomedical materials.

Acknowledgements

The partial financial support by Qatar University is thankfully acknowledged.

Notes and references

1 S. Y. Park, K. T. Oh, Y. T. Oh, N. M. Oh, Y. S. Youn and E. S. Lee, *Chem. Commun.*, 2012, **48**, 2522–2524.
2 K. A. K. Musa and L. Eriksson, *Phys. Chem. Chem. Phys.*, 2009, **11**, 4601–4610.
3 A. D. Bani-Yaseen and M. Al-Balawi, *Phys. Chem. Chem. Phys.*, 2014, **16**, 15519–15526.
4 B. Epe, *Photochem. Photobiol. Sci.*, 2012, **11**, 98–106.
5 R. K. Hans, N. Agrawal, K. Verma, R. B. Misra, R. S. Ray and M. Farooq, *Food Chem. Toxicol.*, 2008, **46**, 1653–1658.
6 A. Albini and S. Monti, *Chem. Soc. Rev.*, 2003, **32**, 238.
7 A. Dawoud Bani-Yaseen, *J. Fluoresc.*, 2011, **21**, 1061–1067.
8 A. D. Bani-Yaseen, F. Hammad, B. S. Ghanem and E. G. Mohammad, *J. Fluoresc.*, 2013, 93–101.
9 N. Chattopadhyay, C. Serpa, L. G. Arnaut and S. J. Formosinho, *Phys. Chem. Chem. Phys.*, 2001, **3**, 3690–3695.
10 F. Bosca, S. Encinas, P. F. Heelis and M. A. Miranda, *Chem. Res. Toxicol.*, 1997, **10**, 820–827.
11 D. E. Moore, S. Roberts-Thomson, D. Zhen and C. C. Duke, *Photochem. Photobiol.*, 1990, **52**, 685–690.
12 S. Encinas, F. Bosca and M. A. Miranda, *Photochem. Photobiol.*, 1998, **68**, 640–645.
13 G. Vredenburg, N. S. Elias, H. Venkataraman, D. F. G. Hendriks, N. P. E. Vermeulen, J. N. M. Commandeur and J. C. Vos, *Chem. Res. Toxicol.*, 2014, **27**, 576–586.
14 G.-J. Cheng, X. Zhang, L. W. Chung, L. Xu and Y.-D. Wu, *J. Am. Chem. Soc.*, 2015, **137**, 1706–1725.
15 J. L. Bolliger, T. K. Ronson, M. Ogawa and J. R. Nitschke, *J. Am. Chem. Soc.*, 2014, **136**, 14545–14553.
16 J. Cerezo, F. J. Avila Ferrer, G. Prampolini and F. Santoro, *J. Chem. Theory Comput.*, 2015, **11**, 5810–5825.
17 A. Dawoud Bani-Yaseen, T. Kawaguchi and R. Jankowiak, *Int. J. Nanomanuf.*, 2009, **43434**, 99–107.
18 M. Schmitt-Jansen, P. Bartels, N. Adler and R. Altenburger, *Anal. Bioanal. Chem.*, 2007, **387**, 1389–1396.
19 S. Encinas, F. Bosca and M. A. Miranda, *Chem. Res. Toxicol.*, 1998, **11**, 946–952.

20 A. Lewandowska, G. L. Hug, G. Hörner, T. Pedzinski, P. Filipiak and B. Marciniak, *ChemPhysChem*, 2010, **11**, 2108–2117.
21 M. Salamone, G. A. DiLabio and M. Bietti, *J. Am. Chem. Soc.*, 2011, **133**, 16625–16634.
22 Y. Yang, L. Liu, J. Chen and K. Han, *Phys. Chem. Chem. Phys.*, 2014, **16**, 17828–17834.
23 G. Litwinienko and K. U. Ingold, *Acc. Chem. Res.*, 2007, **40**, 222–230.
24 J. Peuravuori, *Int. J. Environ. Anal. Chem.*, 2012, **92**, 1470–1492.
25 J. Eriksson, J. Svanfelt and L. Kronberg, *Photochem. Photobiol.*, 2010, **86**, 528–532.
26 H. Görner, *J. Photochem. Photobiol., A*, 2010, **211**, 1–6.
27 A. Achilleos, E. Hapeshi, N. P. Xekoukoulotakis, D. Mantzavinos and D. Fatta-Kassinos, *Chem. Eng. J.*, 2010, **161**, 53–59.
28 S. Bae, D. Kim and W. Lee, *Appl. Catal., B*, 2013, **134–135**, 93–102.
29 S. Canonica, L. Meunier and U. von Gunten, *Water Res.*, 2008, **42**, 121–128.
30 E. Arany, J. Láng, D. Somogyvári, O. Láng, T. Alapi, I. Ilisz, K. Gajda-Schrantz, A. Dombi, L. Kőhidai and K. Hernádi, *Sci. Total Environ.*, 2014, **468–469**, 996–1006.
31 M. J. Frisch, G. W. Trucks, H. B. Schlegel, G. E. Scuseria, M. A. Robb, J. R. Cheeseman, G. Scalmani, V. Barone, B. Mennucci, G. A. Petersson, H. Nakatsuji, M. Caricato, X. Li, H. P. Hratchian, A. F. Izmaylov, J. Bloino, G. Zheng, J. L. Sonnenberg, M. Hada, M. Ehara, K. Toyota, R. Fukuda, J. Hasegawa, M. Ishida, T. Nakajima, Y. Honda, O. Kitao, H. Nakai, T. Vreven, J. A. Montgomery Jr, J. E. Peralta, F. Ogliaro, M. Bearpark, J. J. Heyd, E. Brothers, K. N. Kudin, V. N. Staroverov, R. Kobayashi, J. Normand, K. Raghavachari, A. Rendell, J. C. Burant, S. S. Iyengar, J. Tomasi, M. Cossi, N. Rega, J. M. Millam, M. Klene, J. E. Knox, J. B. Cross, V. Bakken, C. Adamo, J. Jaramillo, R. Gomperts, R. E. Stratmann, O. Yazyev, A. J. Austin, R. Cammi, C. Pomelli, J. W. Ochterski, R. L. Martin, K. Morokuma, V. G. Zakrzewski, G. A. Voth, P. Salvador, J. J. Dannenberg, S. Dapprich, A. D. Daniels, Ö. Farkas, J. B. Foresman, J. V. Ortiz, J. Cioslowski and D. J. Fox, *Gaussian 09, Revision E.01*, Gaussian, Inc., Wallingford, CT, 2009.
32 J. J. P. Stewart, *MOPAC2016, Version: 16.076W*, Stewart Computational Chemistry, 2016, http://OpenMOPAC.net.
33 J. Tomasi, B. Mennucci and E. Cancès, *THEOCHEM*, 1999, **464**, 211–226.
34 C. A. Parker and W. J. Barnes, *Analyst*, 1957, **82**, 606.
35 E. BOWEN and J. ELAND, *Proc. Chem. Soc., London*, 1963, 202.
36 G. Fischer, E. Fischer, K. H. Grellmann, H. Linschitz and A. Temizer, *J. Am. Chem. Soc.*, 1974, **96**, 6267–6269.
37 R. Rahn, J. Schroeder, J. Troe and K. H. Grellmann, *J. Phys. Chem.*, 1989, **93**, 7841–7846.
38 K. Grellmann, W. Kuhnle and H. Weller, *J. Am. Chem. Soc.*, 1981, **103**, 6889–6893.
39 A. Griesbeck, M. Oelgemöller and F. Ghetti, *CRC Handbook of Organic Photochemistry and Photobiology, Third Edition-Two Volume Set-CRC Press Book*, CRC Press, 2nd edn, 2004.
40 L. C. Gilday, S. W. Robinson, T. A. Barendt, M. J. Langton, B. R. Mullaney and P. D. Beer, *Chem. Rev.*, 2015, **115**, 7118–7195.
41 R. Puttreddy, O. Jurček, S. Bhowmik, T. Mäkelä and K. Rissanen, *Chem. Commun.*, 2016, **52**, 2338–2341.
42 Y.-X. Lu, J.-W. Zou, J.-C. Fan, W.-N. Zhao, Y.-J. Jiang and Q.-S. Yu, *J. Comput. Chem.*, 2009, **30**, 725–732.
43 M. R. Scholfield, C. M. Vander Zanden, M. Carter and P. S. Ho, *Protein Sci.*, 2013, **22**, 139–152.
44 R. Wilcken, M. O. Zimmermann, A. Lange, A. C. Joerger and F. M. Boeckler, *J. Med. Chem.*, 2013, **56**, 1363–1388.
45 M. R. Wester, E. F. Johnson, C. Marques-Soares, S. Dijols, P. M. Dansette, D. Mansuy and C. D. Stout, *Biochemistry*, 2003, **42**, 9335–9345.
46 D. A. Pfaff, K. M. Clarke, T. A. Parr, J. M. Cole, B. H. Geierstanger, D. C. Tahmassebi and T. J. Dwyer, *J. Am. Chem. Soc.*, 2008, **130**, 4869–4878.
47 L. Liu, D. Yang and P. Li, *J. Phys. Chem. B*, 2014, **118**, 11707–11714.
48 C. B. Aakerö, T. K. Wijethunga and J. Desper, *Ind. News Ed. J. Indian Chem. Soc.*, 2015, **39**, 757–1528.
49 G.-J. Zhao and K.-L. Han, *Acc. Chem. Res.*, 2012, **45**, 404–413.
50 G.-J. Zhao and K.-L. Han, *Biophys. J.*, 2008, **94**, 38–46.
51 G. J. Zhao and K. L. Han, *J. Phys. Chem. A*, 2007, **111**, 2469–2474.
52 L. P. Kuhn, *J. Am. Chem. Soc.*, 1952, **74**, 2492–2499.
53 S. Hammerum, *J. Am. Chem. Soc.*, 2009, **131**, 8627–8635.
54 W. H. Thompson and J. T. Hynes, *J. Am. Chem. Soc.*, 2000, **122**, 6278–6286.

